Clathrochelate monoribbed-functionalized iron(II) α-dioximates: synthetic pathways and structural and electrochemical features †

Yan Z. Voloshin,*[a] Valery E. Zavodnik,[a] Oleg A. Varzatskii,[b] Vitaly K. Belsky,[a] Aleksei V. Palchik,[b] Nataly G. Strizhakova,[b] Ivan I. Vorontsov[c] and Mikhail Yu. Antipin[c]

[a] *Karpov Institute of Physical Chemistry, 10 Vorontsovo Pole, 103064 Moscow, Russia.*
  E-mail: voloshin@cc.nifhi.ac.ru
[b] *Vernadskii Institute of General and Inorganic Chemistry, 252142 Kiev, Ukraine*
[c] *Nesmeyanov Institute of Organoelement Compounds, 117813 Moscow, Russia*

Monoribbed-functionalized (*i.e.* functionalization of only one of the three α-dioximate fragments) clathrochelate iron(II) tris-dioximates have been synthesized starting from the dichloride precursor $FeBd_2(Cl_2Gm)(BF)_2$ (where Bd^{2-} and Cl_2Gm^{2-} are α-benzyldioxime and dichloroglyoxime dianions, respectively), obtained by condensation of the macrocyclic iron(II) bis-α-benzyldioximate $[FeBd_2(BF_2)_2(MeCN)_2]$ with H_2Cl_2Gm. Thioalkyl, alkylamine, oxo- and azaoxocrown ether clathrochelates, as well as the bis-clathrochelate with a 1,5-diaminopentane bridging fragment, have been characterized using elemental analysis, PD mass, IR, UV-vis, ^{57}Fe Mössbauer and ^1H, ^{13}C and ^{11}B NMR spectroscopies, and X-ray crystallography [for the $FeBd_2(Cl_2Gm)(BF)_2 \cdot 2C_6H_6$, $FeBd_2\{(Et_2N)ClGm\}(BF)_2 \cdot C_6H_6$ and $FeBd_2\{(MeS)_2Gm\}(BF)_2$ complexes]. Configurations intermediate between trigonal prismatic and trigonal antiprismatic have been deduced for the low-spin iron(II) ion coordination polyhedra of the monoribbed-functionalized clathrochelates using ^{57}Fe Mössbauer parameters. The products of de- and re-alkylation reactions of the methylthiol complex $FeBd_2\{(MeS)_2Gm\}(BF)_2$ have been identified. The correlation of $E_{1/2}$ values for Fe^{3+}/Fe^{2+} couples (from cyclic voltammograms) with Hammett σ_{para} constants for substituents in the functionalized fragments is discussed.

Introduction

Clathrochelate ribbed-functionalized tris-dioximates have attracted interest as they offer scope for the synthesis of poly-nuclear complexes with targeted structural parameters and physicochemical properties (especially redox characteristics).[1,2] However, in most instances it is not necessary to functionalize all α-dioximate fragments, and it appears to be sufficient to modify only one of the three ribs in the clathrochelate framework to alter its properties significantly. In particular, such an approach is thought to be promising in creating new types of DNA cleavage agents, since in order to intercalate a complex into a DNA double helix, only one chelate fragment needs to be functionalized.[3] For example, in the majority of ruthenium(II) tris-phenanthroline and tris-bipyridine complexes, intensively studied in recent years in this respect, only one of the three ligand fragments contains functional groups that exert an appreciable and directed influence on the physicochemical characteristics of the whole molecule.[4–10]

In the strong field of the macrobicyclic tris-dioximate ligands, Fe^{2+}, Co^{3+}, Co^{2+} and Ru^{2+} ions have low-spin electronic configurations, short M–N distances and form clathrochelates with similar geometry and chemical properties.[11–18] However, the Fe^{2+} ion has proved to be the most accessible and efficient template in the synthesis of macrobicyclic tris-dioximate complexes.[19,20] It is obvious that pathways developed for obtaining ribbed-functionalized iron(II) clathrochelates and reactions for modifying them should be employable without significant changes for the synthesis of the corresponding complexes of the other ions mentioned.

Results and discussion

Synthesis

Several feasible synthetic routes to clathrochelate monoribbed-functionalized tris-dioximates are shown in Scheme 1. It was established previously[21] that a direct template condensation of a mixture of α-dioximes with Lewis acids on a metal ion (route I) led to the formation of a poorly separable mixture of nonsymmetric and symmetric products, in which the latter predominate. Halogenation of the initial clathrochelate monoglyoxime **1** (route II) is complicated, since by-products are readily generated from partial halogenation of a glyoximate moiety, and the aliphatic and aromatic substituents in the two other dioximate fragments as well. The methods of preparation developed for C_3-nonsymmetric clathrochelates[21] may be used for the synthesis of tris-dioximates **2** and **3** from square-planar macrocyclic bis-dioximates (type **4**) and would seem to be the most promising (routes III and IV). Route III makes use of the condensation of the functionalized α-dioxime with the previously mentioned bis-complex. However, the appearance of additional coordinating groups and side reactions associated with them dramatically reduces the yield of the desired product. Route IV is free from all these disadvantages. The first stage produces a reactive dihalogenide precursor **2** that readily undergoes modification by well-known procedures, hence, this route was chosen for the synthesis of a series of monoribbed-functionalized clathrochelate iron(II) dioximates. The synthesis of the dichloride precursor **6** was carried out *via* the first stage from dichloroglyoxime (H_2Cl_2Gm) and macrocyclic iron(II) bis-α-benzyldioximate **5** [reaction (1)]. Complex **5** was chosen as the starting compound because of its availability and relative stability to disproportionation, yielding symmetric $FeBd_3(BF)_2$ clathrochelate, a product favoured by the steric effects of the bulky phenyl substituents.

DOI: 10.1039/b107021p

*J. Chem. Soc., Dalton Trans.*, 2002, 1193–1202 **1193**
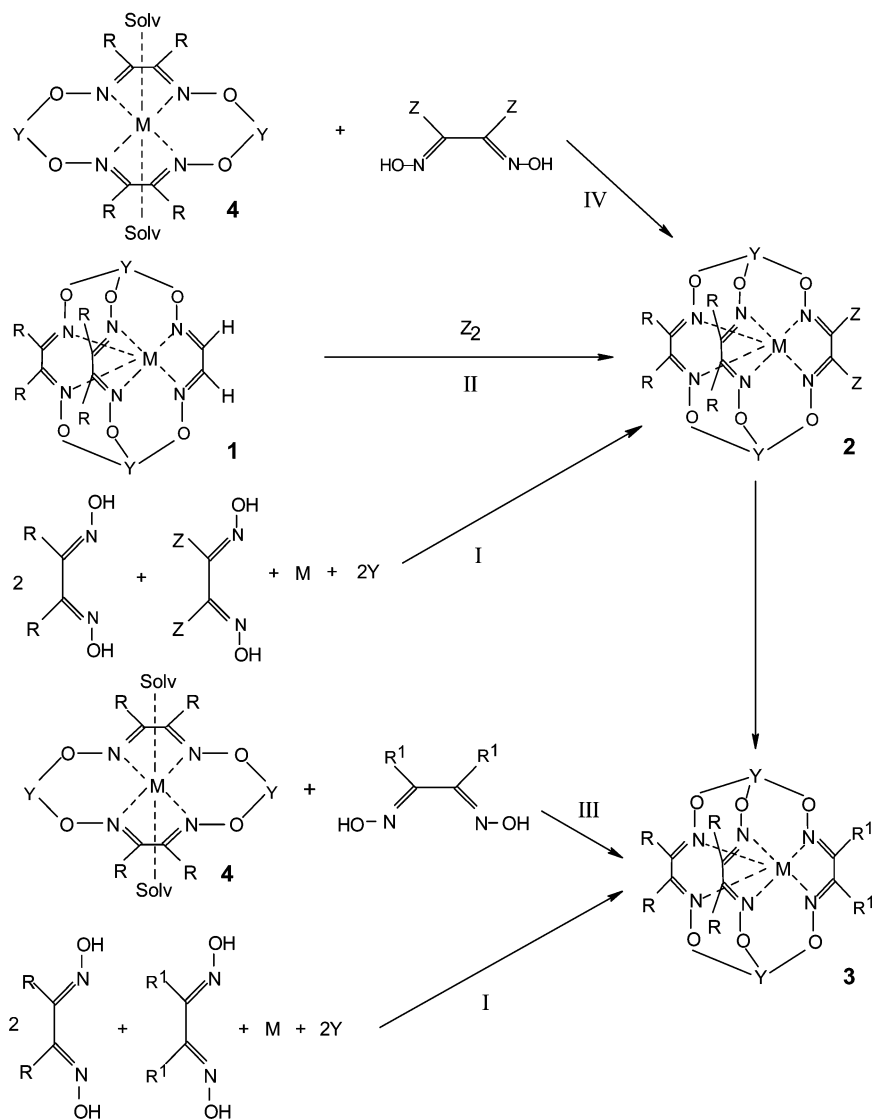
Scheme 1
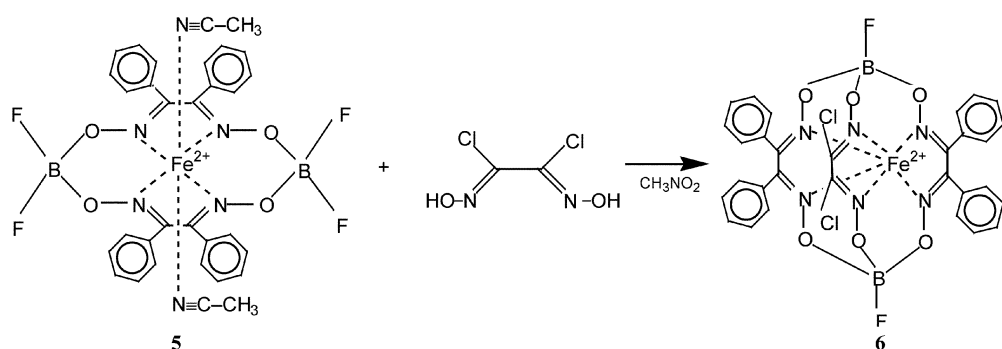
(1)

The dichloride precursor readily reacted with sterically unhindered primary amines (*n*-butylamine in particular) to form disubstituted products (**7**). Secondary amines underwent a reaction that involved substitution of only one of the two chlorine atoms. The reaction of precursor **5** with an excess of aza-18-crown-6 (aza-18-C-6) and diethylamine resulted in the formation of the monocrown-substituted clathrochelate **8** and the monodiethylamine-containing complex **9**. An attempt to isolate the corresponding disubstituted complexes was not successful. The monofunctionalized complexes **8** and **9** may undergo further functionalization, especially with primary aliphatic amines. The use of primary aliphatic diamines enables the functionalized spacer-containing clathrochelate **10** and the bis-clathrochelate **11** (Scheme 2) to be obtained.
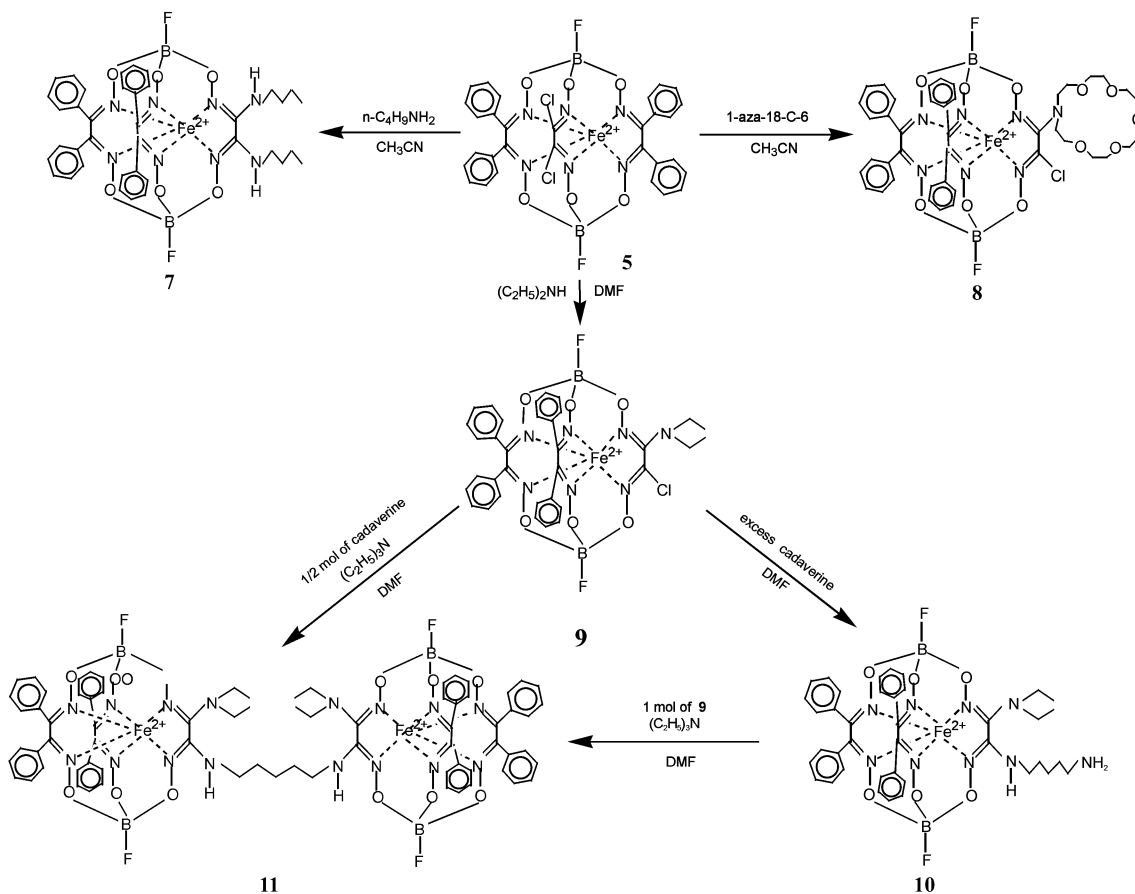
Scheme 2

The synthesis of the functionalized macrobicyclic compound **12**, containing one crown ether dioximate fragment (Cw), was carried out according to reaction (2) using the approach proposed previously for triribbed-functionalized clathrochelates.[1]

Reaction (3) of the precursor **5** with potassium aliphatic thiolates such as MeSK and n-C$_8$H$_{17}$SK was complicated by side reactions, namely the stepwise dealkylation of the resulting

products in an excess of the thiolate ion. This process occurred most readily for the methylthiol derivative **13** [reaction (4)].

Complex **13** also readily underwent de- and re-alkylation, especially with the n-octylthiolate ion (n-OctS) in DMF (Scheme 3).

The products of de- and re-alkylation reactions of clathrochelate **13** were identified by PD and FAB MS techniques. The purification can be improved and the yield of the desired

(2)

(3)

(4)

13

Scheme 3
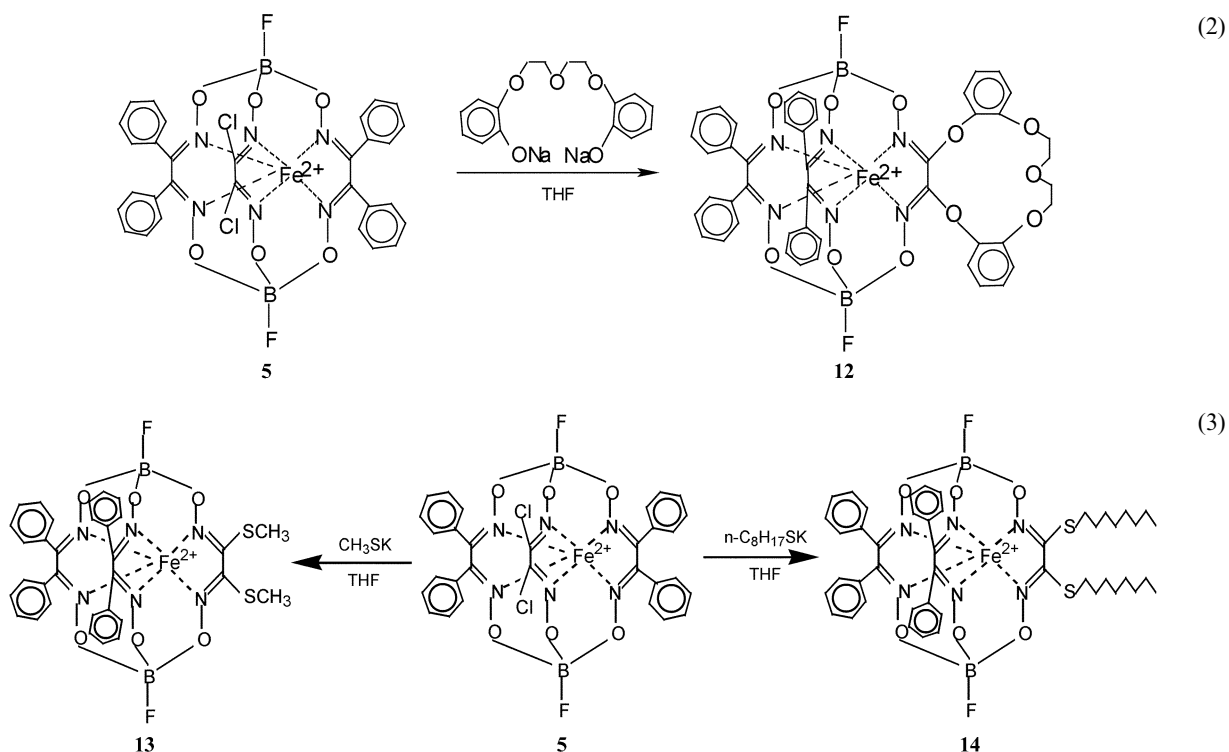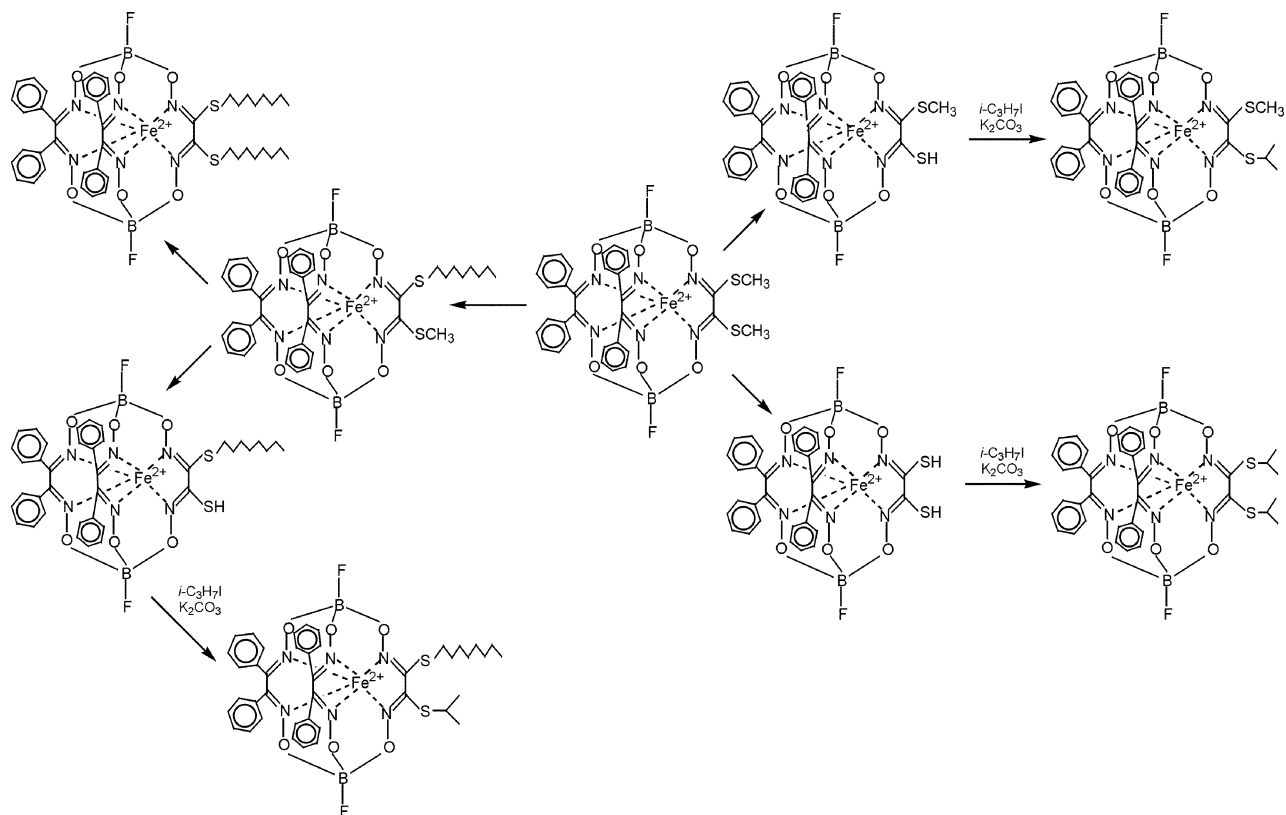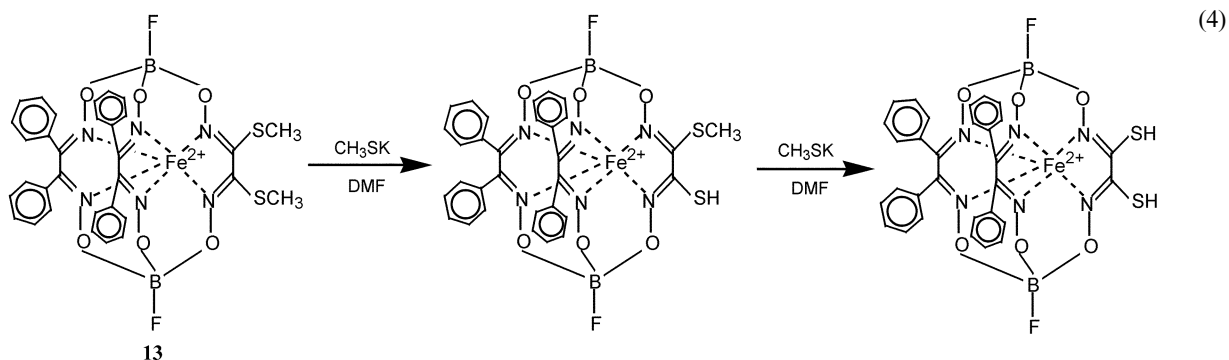
product increased by addition of the corresponding alkyl iodide at the final stage of this process.

Crystal and molecular structures

A summary of the X-ray data for the precursor **6** (Fig. 1) and the functionalized complexes **9** and **13** (Figs. 2 and 3) along with those for their symmetric and C_3-nonsymmetric analogs are presented in Table 1.

It should be noted first of all that the distortion angle φ (approximately 25–27°) of the iron(II) coordination polyhedron [$\varphi = 0°$ for a trigonal prism (TP) and $\varphi = 60°$ for a trigonal antiprism (TAP)] to a trigonal antiprism for the complexes synthesized is close to that of the symmetric $FeBd_3(BF)_2$ α-benzyldioxime ($\varphi = 29.3°$). This distortion is roughly half-way between a TP and a TAP. Meanwhile the Fe–N distances (approximately 1.91 Å) and bite angles a (half the chelate angle, $ca.$ 39°) in clathrochelates **6**, **9** and **13** are typical for boron-containing iron(II) tris-dioximates.[21–29] As a result, the increased coordination polyhedron distortion angle causes a squeeze along the B–Fe–B axes, and the distance h between the polyhedron bases is minimal in $FeBd_3(BF)_2$, $Fe\{(n\text{-}BuNH)_2\text{-}Gm\}_2(Cl_2Gm)(BPh)_2$, $FeBd_2\{(Et_2N)ClGm\}(BF)_2$ (**9**) and $FeBd_2\{(MeS)_2Gm\}(BF)_2$ (**13**) complexes along with the maximal distortion angle (Table 1).

Fig. 1 View of **6** with displacement ellipsoids drawn at the 40% probability level and labeling scheme. H atoms have been omitted for clarity.

Fig. 2 View of **9** with displacement ellipsoids drawn at the 40% probability level and labeling scheme. H atoms have been omitted for clarity.
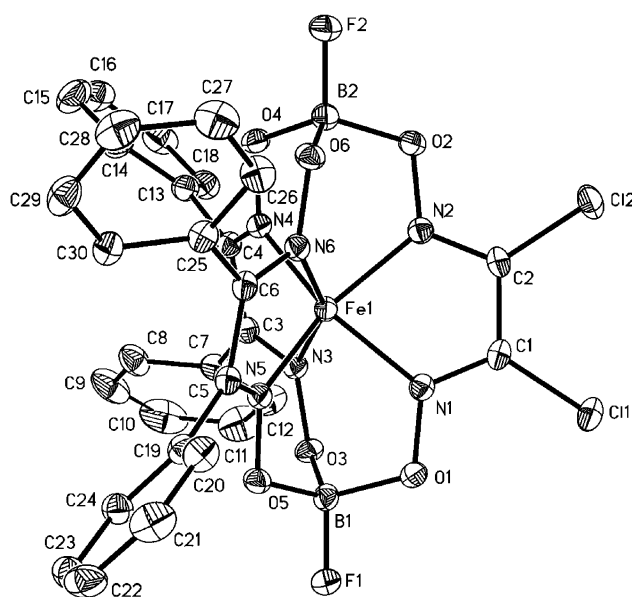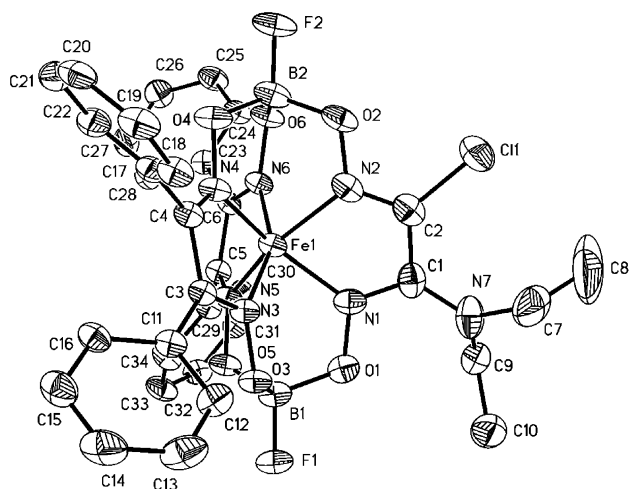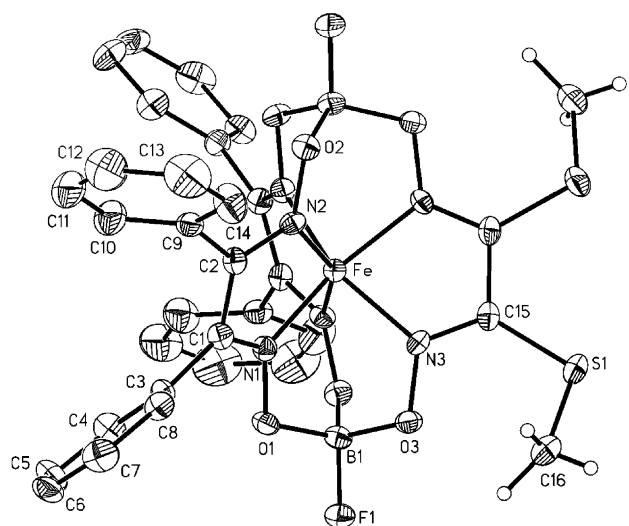

Fig. 3 View of **13** with displacement ellipsoids drawn at the 30% probability level and labeling scheme. H atoms have been omitted for clarity (except hydrogen atoms of methyl groups).

Specific features of the structures for complexes **6** and **9** that should be highlighted are a tendency for the C–C=N angles in the chlorine-containing chelate fragments to have larger values compared to those in phenyl-containing substituents (Table 1). In **9**, the dihedral angle between the plane C7–N7–C9 of the diethylamine group and that of the C1–Fe1–C2 fragment is 37.7(2)°. In the clathrochelates **6**, **9** and **13**, the phenyl substitutents have similar mutual orientations: the dihedral angles between phenyl-substituted and corresponding C–Fe–C fragments are in the range 44.2(4)–60.4(8)° (average ~ 50°). The average inclination of the benzene rings to each other for the same chelate fragment is approximately 53°. Despite the fact that the molecular geometries of these clathrochelates look in some respects alike, their molecular packing arrangements are substantially different (see ESI). There are no specific intermolecular interactions in the structures of **6** and **9**, but the molecular packing of complex **13** is characterized particularly by S ⋯ F intermolecular contacts of 3.120(6) Å (see ESI). The negative thermal expansion of the crystal **9** along the *a* axis in the range 103–160 K should also be noted.

^{57}Fe Mössbauer spectra

Attempts to obtain crystals of other synthesized monoribbed-functionalized complexes suitable for X-ray analysis were not successful. Therefore, to obtain information about their geom-

etry, we utilized the results of indirect methods and, initially, ^{57}Fe Mössbauer spectra. The parameters of these spectra (Table 1) characterize the compounds obtained as low-spin complexes of Fe^{2+} ion in the high field of the clathrochelate ligand. The isomer shift (IS) values, characterizing the s-electron density on the central metal ion nucleus, are practically identical for the synthesized C_3-nonsymmetric clathrochelates and their symmetric analogs, which have been reported previously.[1] The quadrupole splitting (QS), which is determined by the electric field gradient (EFG) on the iron atom nucleus, was used [30,31] to obtain the geometries of the low-spin iron(II) complexes by predicting the magnitude of the distortion angle φ. The QS values for the synthesized C_3-nonsymmetric complexes occupy a position intermediate between the QS values for the corresponding symmetric analogs (after allowing for the influence of a substituent at the boron atom). Replacement of phenyl and *n*-butyl substituents by fluorine in the case of the majority of alicyclic and aliphatic α-dioxime clathrochelates results in an increase in the QS magnitude about 0.1–0.2 mm s^{-1}. The QS values for the clathrochelates, consideration of the X-ray analysis data for the symmetric analogs [1] and for $FeBd_2(Cl_2Gm)(BF)_2 \cdot 2C_6H_6$ (**6**), $FeBd_2\{(Et_2N)ClGm\}(BF)_2 \cdot C_6H_6$ (**9**) and $FeBd_2\{(MeS)_2Gm\}(BF)_2$ (**13**), the correlation relationship "QS *versus* φ",[30] and a modern version of the partial quadrupole splitting concept,[31] allowed the prediction of the distortion angle φ, listed in Table 1. A positive QS sign was postulated for all boron-containing clathrochelates. The geometries of the synthesized complexes were found to be closer to a trigonal prism than that of the $FeBd_3(BF)_2$ clathrochelate.

The slightly increased QS values obtained for the synthesized compounds compared with those expected can be accounted for by the fact that the molecules have no C_3 symmetry axis passing through the apical boron atoms and the central iron ion, and this induces an additional increase in the EFG.

NMR spectra

The ^{1}H and ^{13}C NMR spectra of the complexes (see ESI) contain signals characteristic of both types of dioximate fragments, which (in addition to the ratio of line integral intensities in the ^{1}H NMR and PD mass spectra) confirmed their composition, as well as the presence of a C_2 symmetry axis passing through the middle of the C–C bond in the functionalized chelate ring and the iron atom. The fully nonsymmetric clathrochelates proved to be the only exception; assignment of the signals in their ^{13}C NMR spectra was performed by recording these spectra with and without decoupling of the spin–spin ^{1}H–^{13}C interaction. The ^{11}B NMR spectra of these compounds (see ESI) contain two doublets, governed by the spin–spin ^{11}B–^{19}F interactions, unlike the ^{11}B NMR spectra of other compounds that contain one doublet. The low values of the $J_{^{11}B-^{19}F}$ constant (approximately 15 Hz) are also characteristic of boron atoms in a highly symmetric tetrahedral environment.

UV-vis spectra

A single intense Md → Lπ* charge transfer band (CTB) was evident in the visible region of the UV-vis spectra of the synthesized clathrochelates. However, with certain C_3-nonsymmetric clathrochelates, two bands of nearly identical intensity have been detected in other studies.[21] These arise from metal to ligand charge transfer into the π*-orbitals of different types of dioximate fragments. In all other instances, only one band was observed, with λ_{max} intermediate between the values found for the corresponding symmetric clathrochelate tris-dioximates.[21] An analogous situation was observed for the complexes described herein. The position of the CTB in the UV-vis spectra depends somewhat on the nature of the capping group, and therefore the resemblance between the λ_{max} values of the compounds synthesized and those of the $FeBd_3(BF)_2$

1198

J. Chem. Soc., Dalton Trans., 2002, 1193–1202

Table 1 Parameters of [57]Fe Mössbauer spectra and the main X-ray data for the complexes obtained and their analogs

| Compound | ^{57}Fe Mössbauer data | | | X-Ray crystallographic data | | | | | | | | | | | |
| | IS/mm s^{-1} | QS/mm s^{-1} | φ found (calc.)/° | | | | Average structural parameters of chelating fragments | | | | | Average structural parameters of capping fragments | | | |
				h^a/Å	a^b/°	$\varDelta^c$/Å	N=C–C=N^d/°	Fe–N/Å	C–C/Å	C=N/Å	C–C=N/°	N–O/Å	B–O/Å	O–B–C (O–B–F)/°	O–B–O/°
Fe(Cl₂Gm)₃(BF)₂·2THF [1]	0.37	0.64	17.1	2.36	39.0	0.083	8.1	1.91	1.429	1.276	112.3	1.370	1.464	108.0	110.9
Fe{(n-BuNH)₂Gm}₂(Cl₂Gm)(BPh)₂ (type A) [1]	0.38	0.69	27.3	2.33	39.5	0.102	9.8	1.92	1.427	1.306	111.5	1.362	1.500	108.7	110.2
					40.3 (Cl₂Gm) 39.0 (N₂Gm)	0.282	26.8 (Cl₂Gm)	1.89 (Cl₂Gm) 1.96 (N₂Gm)	1.458 (Cl₂Gm)	1.305 (N₂Gm)		1.396 (Cl₂Gm)			
Fe{(n-BuNH)₂Gm}₂(Cl₂Gm)(BPh)₂ (type B) [1]	0.38	0.69	29.2	2.30	39.5	0.105	10.0	1.91	1.435	1.304	111.3	1.367	1.490	108.4	110.7
					40.4 (Cl₂Gm) 39.0 (N₂Gm)	0.203 0.206	19.2 (Cl₂Gm) 19.6 (N₂Gm)	1.89 (Cl₂Gm) 1.93 (N₂Gm)	1.476 (Cl₂Gm)	1.291 (N₂Gm)		1.400 (Cl₂Gm)			
FeBd₃(BF)₂ [22]	0.32	0.25	29.3	2.29	39.3	0.15	13.8	1.91	1.51	1.25 1.32	110	1.38	1.49	107	112
FeBd₂(Cl₂Gm)(BF)₂·2C₆H₆ (6)	0.35	0.62	24.8	2.33	39.3	0.08 0.08 (Cl₂Gm) 0.08 (Ph₂Gm)	7.7(2) 7.6(2) (Cl₂Gm) 7.8(2) (Ph₂Gm)	1.909(1) 1.913(1) (Cl₂Gm) 1.908(1) (Ph₂Gm)	1.435(2) 1.456(2) (Cl₂Gm)	1.301(2) 1.312(2) (Cl₂Gm)	112.6(1) 111.1(1) (Cl₂Gm)	1.370(2)	1.486(2)	108.0(2)	110.9(2)
FeBd₂{(Et₂N)ClGm}(BF)₂·C₆H₆ (9)	0.34	0.31	26.6	2.31	39.3	0.09 (ClGm) 0.10 (NGm) 0.12 (Ph₂Gm)	9.2(5) (ClNGm) 10.6(5) (Ph₂Gm)	1.909(3) (ClNGm) 1.924(3) (ClGm) 1.924(3) (NGm) 1.900(3)	1.447(6) (ClNGm) 1.464(6) (ClGm)	1.323(5) (NGm) 1.281(5) (ClGm) 1.309(5) (Ph₂Gm)	109.7(4) (NGm) 113.9(4) (ClGm) 110.8(4) (Ph₂Gm)	1.374(4)	1.483(6)	107.9(4)	111.2(3)
FeBd₂{(MeS)₂Gm}(BF)₂ (13)	0.32	0.36	25.8	2.31	39.3	0.05 (Ph₂Gm) 0.07 (S₂Gm)	3.9 (Ph₂Gm) 6.7 (S₂Gm)	1.902(5) (Ph₂Gm) 1.898(5) (Ph₂Gm) 1.910(8) (S₂Gm)	1.42(1) (Ph₂Gm) 1.46(1) (S₂Gm)	1.321(8) (Ph₂Gm) 1.283(8) (S₂Gm)	111.8(6) (Ph₂Gm) 111.7(4) (S₂Gm)	1.373(7)	1.479(9)	107.0(6)	111.8(5)
FeBd₂{(n-BuNH)₂Gm}(BF)₂ (7)	0.35	0.76	(24–29)												
FeBd₂{(aza18-C-6)ClGm}(BF)₂ (8)	0.34	0.45	(24–29)												
FeBd₂{(Et₂N)[NH₂(CH₂)₅NH]Gm}-(BF)₂ (10)	0.34	0.53	(24–29)												
[FeBd₂{(Et₂N)Gm}(BF)₂]₂NH(CH₂)₅-NH (11)	0.34	0.47	(24–29)												
FeBd₂(CwGm)(BF)₂ (12)	0.36	0.50	(24–29)												
FeBd₂{(n-OctS)₂Gm}(BF)₂ (14)	0.32	0.34	(26–31)												

^{a} Distance between the coordination polyhedron bases (the height of the distorted trigonal prism). ^{b} Bite angle (half the chelate angle). ^{c} Mean deviation of the coordinated nitrogen atoms from the C–Fe–C plane. ^{d} Dihedral angles for the chelating fragments.

Table 2 The electrochemical characteristics of clathrochelate iron(II) α-benzyldioximates (in CH_2Cl_2)

Compound	$\sigma_I{}^a$		$\sigma_{para}{}^a$		$E_{1/2}/$ mV	Tomeš criterion/ mV
$FeBd_2(Cl_2Gm)(BF)_2$ (**6**)	0.47		0.227		1100	70
$FeBd_2\{(n\text{-}BuNH)_2Gm\}(BF)_2$ (**7**)	0.10		−0.63		400	75
					375[b]	60[b]
$FeBd_2\{(aza18\text{-}C\text{-}6)ClGm\}(BF)_2$ (**8**)	0.06 (aza)	} 0.26	−0.95 (aza)	} −0.36	720	56
	0.47 (Cl)		0.227 (Cl)			
$FeBd_2\{(Et_2N)ClGm\}(BF)_2$ (**9**)	0.47 (Cl)	} 0.26	0.227 (Cl)	} −0.36	720	56
	0.06 (Et$_2$N)		−0.95(Et$_2$N)			
$FeBd_2\{(Et_2N)[NH_2(CH_2)_5NH]Gm\}(BF)_2$ (**10**)	0.06 (Et$_2$N)	} 0.08	−0.95 (Et$_2$N)	} −0.79	430	56
	0.10 [NH(CH$_2$)$_5$NH$_2$]		−0.63 [NH(CH$_2$)$_5$NH$_2$]			
$[FeBd_2\{(Et_2N)Gm\}(BF)_2]_2NH(CH_2)_5NH$ (**11**)	0.06 (Et$_2$N)	} 0.08	−0.95 (Et$_2$N)	} −0.79	450	56
	0.10 [NH(CH$_2$)$_5$NH]		−0.63 [NH(CH$_2$)$_5$NH]			
$FeBd_2(CwGm)(BF)_2$ (**12**)	0.38		−0.32		800	90
$FeBd_2\{(MeS)_2Gm\}(BF)_2$ (**13**)	0.19		0.00		880	70
$FeBd_2\{(n\text{-}OctS)_2Gm\}(BF)_2$ (**14**)	0.17		−0.06		920	100
					890[b]	60[b]
$FeBd_2Gm(BF)_2$	0		0		1040	65
$FeBd_2Nx(BF)_2{}^c$	−0.05		−0.15		890	56
$FeBd_3(BF)_2{}^{21,c}$	0.10		−0.01		925	100
					940[b]	70[b]
$FeBd_2Dm(BF)_2{}^{21}$	−0.05		−0.17		875	60
					900[b]	70[b]

^{a} Taft (σ_I) and Hammett (σ_{para}) constants for substituents in α-dioximate fragments. $\sigma_\Sigma = [n/(m + n)]\sigma_1 + [m/(m + n)]\sigma_2$, $\sigma_{n + 1} = \sigma_n/2.5$. ^{b} Data for solution in acetonitrile. ^{c} Nx^{2-} and Dm^{2-} are cyclohexanedion-1,2-dioxime (nioxime) and dimethylglyoxime dianions, respectively.

complex is obvious, unlike the λ_{max} values for the triribbed-functionalized clathrochelates. This indicates that the influence of two diphenylglyoximate fragments on the electronic system of a highly conjugated macrobicyclic ligand predominates over that of the functionalized fragment.

Electrochemistry

Most of the clathrochelates synthesized undergo quasi-reversible or irreversible oxidations, which are comparable to those observed for other clathrochelate iron(II) complexes. They are assigned to metal-based $Fe^{3+/2+}$ redox couples.[1,11,13,14] Their electrochemical properties are characterized by the half-wave potential value, $E_{1/2}$, which depends on the electron-donating properties of the substituents both in the capping groups and α-dioximate fragments. Table 2 lists these $E_{1/2}$ values for various clathrochelates as well as the Tomeš criterion values (ΔE), which characterize the reversibility of an electrochemical process (the Tomeš criterion is determined as $\Delta E = E_{3/4} - E_{1/4}$ and for a one-electron reversible process, this value is equal to 56 mV at 298 K [32–34]).

As can be seen from Table 2, the oxidation process for most of the fluoroboron-containing clathrochelates is reversible ($\Delta E = 56\text{–}60$ mV) or quasi-reversible ($\Delta E = 65\text{–}75$ mV). For these complexes, except $FeBd_2(Cl_2Gm)(BF)_2$ (**6**) and $FeBd_2Gm(BF)_2$, the reduction waves were observed on reversing the potential scan. Both direct and reverse waves were reproduced under repeated cycling. However, the $FeBd_2(Cl_2Gm)(BF)_2$ (**6**) and $FeBd_2Gm(BF)_2$ clathrochelate oxidation processes were accompanied by destruction of the oxidation products, since there were no reverse waves were observed in the voltammograms, moreover, the working electrode was also passivated.

The complexes $FeBd_2(CwGm)(BF)_2$ (**12**), $FeBd_2\{(n\text{-}OctS)_2\text{-}Gm\}(BF)_2$ (**14**) and $FeBd_3(BF)_2$ also oxidised irreversibly in methylene dichloride, which was evident from both the Tomeš criterion values (90–100 mV) and from the absence of reverse waves. However, a reverse wave for the $FeBd_2\{(n\text{-}OctS)_2Gm\}$-$(BF)_2$ (**14**) complex was registered in acetonitrile, and both direct and reverse waves were reproducible. Thus, the stability of the oxidation product in acetonitrile is clearly higher than that in methylene dichloride (in cyclic voltammetry time scale).

The $E_{1/2}$ values for the complexes correlate reasonably well with the Hammett σ_{para} constants of substituents in the
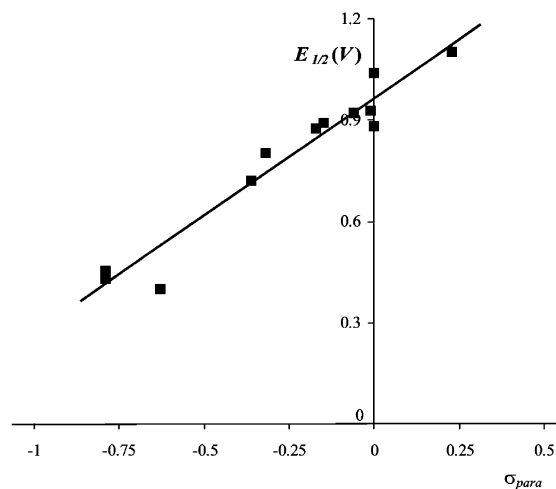

Fig. 4 Correlation of $E_{1/2}$ for Fe^{3+}/Fe^{2+} couples of the monoribbed-functionalized fluoroboronic clathrochelates with the Hammett σ_{para} constants for the substituents in the functionalized α-dioximate fragments.

functionalized fragment (the correlation coefficient is 0.94; Fig. 4), though there was no correlation between the $E_{1/2}$ values and the inductive Taft σ_I constants.

Experimental

General procedures

The reagents used, $FeCl_2\cdot4H_2O$, α-benzyldioxime (H_2Bd), C_6H_5SH, MeSH, $BF_3\cdot OEt_2$, sorbents, 1-aza-18-crown-6 (abbreviated as aza-18-C-6), 1,5-diaminopentane (cadaverine), organic bases and their salts, and organic solvents were obtained commercially (Fluka). Bis[2-(o-oxyphenoxy)]diethyl ether and the $[Fe(HBd)_2py_2]$ complex were prepared as described in refs. 35 and 36, respectively. The dichloroglyoxime (denoted as H_2Cl_2Gm) was obtained by chlorination of glyoxime (H_2Gm) as described in ref. 37.

Analytical data (C, H, N content) were obtained with a Carlo Erba model 1106 microanalyzer. Iron content was determined spectrophotometrically.

The plasma desorption (PD) mass spectra were recorded in the positive spectral range using a BC MS SELMI time-of-flight biochemical mass spectrometer and an accelerating voltage of 20 kV. The ionization was induced by ^{252}Cf spontaneous decay fragments, and typically 20 000 decay acts were registered. The samples (approximately 1–2 mg) were applied to a gilded disk or a nitrocellulose layer.

The IR spectra of solid samples (KBr tablets) in the range 400–4000 cm^{-1} were recorded with a Specord M-80 Carl Zeiss spectrophotometer.

UV-vis spectra of solutions in chloroform were recorded in the range 230–800 nm with a Lambda 9 Perkin Elmer spectrophotometer. The individual Gauss components of these spectra were calculated using the SPECTRA program.[38]

The ^{1}H, ^{13}C and ^{11}B NMR spectra were recorded from CDCl$_3$ solutions with a Bruker AC-200 FT-spectrometer.

^{57}Fe Mössbauer spectra were obtained with a YGRS-4M spectrometer with a constant acceleration mode. The spectra were collected with a 256-multichannel amplitude analyzer. The isomer shift was measured relative to sodium nitroprusside, and an α-Fe foil was used for the velocity scale calibration. ^{57}Co in a Cr matrix was used as the source, which was always kept at room temperature. The minimal absorption line-width in the spectrum of a standard sample of sodium nitroprusside was 0.24 mm s^{-1}.

Cyclic voltammograms were recorded in methylene dichloride and acetonitrile under argon using a PI-50-1 potentiostat coupled with a B7-45 tera-ohmic potentiometer as the current voltage convertor. The scan rate was varied from 5 to 10 mV s^{-1}, which is close to the steady-state conditions for ultramicro-electrodes.[34] Tetraethylammonium tetrafluoroborate (0.1 M) was used as the supporting electrolyte. A platinum micro-electrode 10 μm in diameter, thoroughly polished and rinsed before measurements, was chosen as the working electrode. A platinum wire was used as the auxiliary electrode. A standard Ag/AgCl reference electrode was connected to the cell *via* a salt bridge. All potentials were referenced to the redox potential of the ferrocene (Fc$^+$/Fc) couple as an internal standard. This potential is at +0.58 (for CH$_2$Cl$_2$ solutions) and +0.45 V (for MeCN solutions) *vs*. Ag/AgCl under the present experimental conditions.

Syntheses

[FeBd$_2$(BF$_2$)$_2$(MeCN)$_2$] (5). This compound was obtained by a procedure similar to that used to prepare the [FeDm$_2$-(BF$_2$)$_2$(MeCN)$_2$] complex.[39]

The complex [Fe(HBd)$_2$py$_2$] (108 g, 156 mmol) was suspended in a dry diethyl ether–acetonitrile mixture (6 : 1, 700 ml) with intensive stirring and freshly distilled BF$_3$·OEt$_2$ (85.4 ml, 690 mmol) was added dropwise under argon. The reaction mixture was stirred for 30 min and filtered. The solid product was washed with diethyl ether (200 ml), acetone–acetonitrile mixture (9 : 1, 1000 ml in five portions), diethyl ether–acetonitrile mixture (20 : 1; 150 ml in three portions), hexane–hexamethyldisiloxane mixture (50 : 1, 100 ml in two portions) and then with hexane (100 ml), and dried *in vacuo*. Yield: 96 g (87%).

FeBd$_2$(Cl$_2$Gm)(BF$_2$)$_2$ (6). Complex **5** (35 g, 50 mmol) and an excess of H$_2$Cl$_2$Gm (9.4 g, 60 mmol) were dissolved/suspended in a dry nitromethane–hexamethyldisiloxane mixture (6 : 1, 175 ml) with intensive stirring under argon. Triethylamine (21 ml, 150 mmol), BF$_3$·OEt$_2$ (18.6 ml, 150 mmol) and chloroform (20 ml) were added dropwise to the reaction mixture. The solution was heated to boiling point and a second portion of BF$_3$·OEt$_2$ (18.6 ml, 150 mmol) was added. Then, 120 ml of solvent was distilled off with intensive stirring and the mixture was allowed to cool to room temperature. The microcrystalline orange solid was filtered off, washed with methanol, diethyl ether and then with hexane, and dried *in vacuo*. Yield: 23 g (63%). Anal. calc. for C$_{30}$H$_{20}$N$_6$O$_6$B$_2$Cl$_2$F$_2$Fe: C, 48.23; H, 2.68; N, 11.25; Cl, 9.51; Fe, 7.48; found: C, 48.21; H, 2.73; N, 11.17; Cl, 9.42; Fe, 7.38%. MS(PD): *m/z* 747 [M]$^{+•}$, 624 [M − Cl$_2$C$_2$N$_2$]$^{+•}$. UV-vis (CHCl$_3$): λ_{max} (10^{-3} ε) 243 (25), 283 (12), 428 (3.4), 469 nm (23 dm^3 mol^{-1} cm^{-1}).

FeBd$_2${(*n*-BuNH)$_2$Gm}(BF)$_2$ (7). Complex **6** (0.75 g, 1 mmol) was suspended in acetonitrile (20 ml), and an excess of *n*-butylamine (1 ml) was added. The reaction mixture was left overnight and then refluxed for 2 h. The resulting dark-red solution was precipitated with a 5-fold volume of water. The solid was filtered off, dried *in vacuo* and dissolved in chloroform. The solution was filtered through Silasorb SPH-300 and evaporated to dryness. Yield: 0.73 g (90%). Anal calc. for C$_{38}$H$_{40}$N$_8$O$_6$B$_2$F$_2$Fe: C, 55.65; H, 4.88; N, 13.67; Fe, 6.81; found: C, 55.71; H, 4.88; N, 13.57; Fe, 6.82%. MS(PD): *m/z* 819 [M]$^{+•}$. UV-vis (CHCl$_3$): λ_{max} (10^{-3} ε) 249 (27), 292 (19), 365 (5.5), 432 (3.4), 506 nm (20 dm^3 mol^{-1} cm^{-1}).

FeBd$_2${(aza18-C-6)ClGm}(BF)$_2$ (8). Complex **6** (0.75 g, 1 mmol) and aza-18-C-6 (0.53 g, 2 mmol) were dissolved/suspended in dry acetonitrile (15 ml) and left overnight. Then, the reaction mixture was refluxed for 3 h and evaporated to 3 ml. Triethylamine (0.5 ml) was added, and the dark-red product was precipitated with methanol (10 ml). The solid was washed with a small amount of diethyl ether, and then with hexane, and dried *in vacuo*. Yield: 0.65 g (70%). Anal calc. for C$_{42}$H$_{44}$N$_7$O$_{11}$B$_2$ClF$_2$Fe: C, 51.80; H, 4.52; N, 10.07; Cl, 3.65; Fe, 5.74; found: C, 51.77; H, 4.52; N, 9.94; Cl, 3.66; Fe, 5.77%. MS(PD): *m/z* 973 [M]$^{+•}$. UV-vis (CHCl$_3$): λ_{max} (10^{-3} ε) 249 (27), 288 (18), 347 (4.5), 484 nm (24 dm^3 mol^{-1} cm^{-1}).

FeBd$_2${(Et$_2$N)ClGm}(BF)$_2$ (9). Complex **6** (0.75 g, 1 mmol) and an excess of diethylamine (0.5 ml) were dissolved/suspended in dry DMF (15 ml) and left overnight. Then the reaction mixture was stirred for 7 h at 50 °C and the resulting dark-orange solution was precipitated with a 2-fold volume of water. The solid was filtered off and reprecipitated from DMF solution with saturated aqueous NaClO$_4$ solution. The resulting orange product was washed with water and a small amount of methanol, and dried *in vacuo*. The solid was dissolved in chloroform, and the solution was filtered through Silasorb SPH-300 and evaporated to dryness. The solid residue was washed with a small amount of chloroform, and then with hexane, and dried *in vacuo*. Yield: 0.32 g (41%). Anal. calc. for C$_{34}$H$_{30}$N$_7$O$_6$B$_2$ClF$_2$Fe: C, 52.11; H, 3.83; N, 12.52; Cl, 4.53; Fe, 7.13; found: C, 51.98; H, 3.81; N, 12.42; Cl, 4.59; Fe, 7.12%. MS(PD): *m/z* 783 [M]$^{+•}$, 748 [M − Cl]$^{+•}$, 624 [M − ClC$_2$-N$_2$NEt$_2$]$^{+•}$. MS(MALDI-TOF): *m/z* 784 [M + H$^+$]$^+$, 806 [M + Na$^+$]$^+$, 822 [M + K$^+$]$^+$. UV-vis (CHCl$_3$): λ_{max} (10^{-3} ε) 254 (28), 294 (14), 338 (4.0), 484 nm (22 dm^3 mol^{-1} cm^{-1}).

FeBd$_2${(Et$_2$N)[NH$_2$(CH$_2$)$_5$NH]Gm}(BF)$_2$ (10). Complex **9** (0.23 g, 0.3 mmol) and an excess of cadaverine (0.7 ml) were dissolved/suspended in dry DMF (10 ml) and left overnight. Then the resulting dark-red solution was precipitated with a 2-fold volume of water. The solid was filtered off and reprecipitated from DMF solution with saturated aqueous NaClO$_4$ solution. The resulting red product was washed with methanol–water (1 : 1) mixture, and dried *in vacuo*. The solid was dissolved in chloroform and the solution was passed through a 30 mm layer of Silasorb SPH-300. The chloroform elute was discarded and the desired complex eluted with acetonitrile–chloroform (1 : 3) mixture. The red solution was evaporated to dryness and dissolved in a small amount of chloroform. The chloroform solution obtained was diluted with a 3-fold volume of hexane and evaporated to dryness. The solid residue was washed with hexane and dried *in vacuo*. Yield: 0.055 g (22%). Anal. calc. for C$_{39}$H$_{43}$N$_9$O$_6$B$_2$F$_2$Fe: C, 55.16; H, 5.07; N, 14.85; Fe, 6.58; found:

Table 3 Crystallographic data and experimental details for FeBd$_2$(Cl$_2$Gm)(BF)$_2$·2C$_6$H$_6$ (**6**), FeBd$_2${(Et$_2$N)ClGm}(BF)$_2$·C$_6$H$_6$ (**9**) and FeBd$_2$-{(MeS)$_2$Gm}(BF)$_2$ (**13**)

Data	6	9	13
Empirical formula	C$_{42}$H$_{32}$B$_2$Cl$_2$F$_2$FeN$_6$O$_6$	C$_{40}$H$_{36}$B$_2$ClF$_2$FeN$_7$O$_6$	C$_{32}$H$_{26}$B$_2$F$_2$FeN$_6$O$_6$S$_2$
Fw	903.11	861.68	770.18
Color, habit	Dark-orange, prism	Dark-orange, prism	Orange–red, prism
Crystal dimensions/mm	0.07 × 0.15 × 0.40	0.50 × 0.50 × 0.20	0.42 × 0.38 × 0.32
Temperature/K	110	120	293
a/Å	14.754(2)	17.077(3)	9.993(1)
b/Å	10.339(1)	21.551(4)	9.993(1)
c/Å	27.126(3)	21.580(4)	34.575(7)
β/°	90.942(2)	90	90
V/Å^3	4137.1(8)	7942(2)	3452.7(9)
Z	4	8	4
Crystal system	Monoclinic	Orthorhombic	Tetragonal
Space group	$P2_1/c$	$Pbca$	$P4_12_12$
D_{calc}/g cm^{-3}	1.450	1.441	1.482
μ/mm^{-1}	0.559	0.514	0.622
Data/restraints/parameters	12081/0/678	9127/0/532	2402/0/231
Weighting scheme	$1/[\sigma^2(F_o^2) + (0.0804P)^2 + 0.1263P]$, $P = (F_o^2 + 2F_c^2)/3$	$1/[\sigma^2(F_o^2) + (0.1243P)^2 + 2.3045P]$, $P = (F_o^2 + 2F_c^2)/3$	$1/[\sigma^2(F_o^2) + (0.1348P)^2 + 3.0994P]$, $P = (F_o^2 + 2F_c^2)/3$
R^a [$I > 2\sigma(I)$]	0.0426	0.0635	0.0560
R_w^b [$I > 2\sigma(I)$]	0.1119	0.1884	0.1696
$F(000)$	1848	3552	1576
GOF^c	1.068	1.206	1.106
Absolute structure parameter	—	—	0.00(4)

^{a} $R = (\Sigma ||F_o| - |F_c||)/\Sigma|F_o|$. ^{b} $R_w = [(\Sigma [w(F_o^2 - F_c^2)^2])/(\Sigma[w(F_o^2)^2])]^{1/2}$. ^{c} GOF $= [(\Sigma [w (F_o^2 - F_c^2)^2])/(N_{obs} - N_{param})]^{1/2}$.

C, 55.18; H, 5.03; N, 14.74; Fe, 6.62%. MS(PD): m/z 848 [M]$^{+\cdot}$. UV-vis (CHCl$_3$): λ_{max} (10^{-3} ε) 243 (26), 296 (11), 343 (4.6), 469 (5.1), 512 nm (14 dm^3 mol^{-1} cm^{-1}).

[FeBd$_2${(Et$_2$N)Gm}(BF)$_2$]$_2$NH(CH$_2$)$_5$NH (11). Complex **9** (0.23 g, 0.3 mmol) was dissolved/suspended in dry DMF (10 ml) and solution of cadaverine (0.018 ml, 0.15 mmol) and triethylamine (0.042 ml, 0.3 mmol) in DMF (5 ml) was added dropwise to the stirred reaction mixture. The reaction mixture was left overnight and then was stirred at 50–60 °C for 3 h. The product was precipitated from the resulting red solution with a 2-fold volume of water and the solid reprecipitated from DMF solution with saturated aqueous NaClO$_4$ solution. The resulting red product was washed with a small amount of methanol and dried *in vacuo*. The solid was dissolved in chloroform and the solution filtered through Silasorb SPH-300 and the orange–red solution evaporated to dryness. The solid residue was washed with hexane and dried *in vacuo*. Yield: 0.06 g (40%). Anal. calc. for C$_{73}$H$_{72}$N$_{16}$O$_{12}$B$_4$F$_4$Fe$_2$: C, 54.93; H, 4.51; N, 14.05; Fe, 7.00; found: C, 54.81; H, 4.48; N, 13.98; Fe, 7.07%. MS(PD): m/z 1595 [M]$^{+\cdot}$. MS(MALDI-TOF): m/z 1596 [M + H$^+$]$^+$, 1618 [M + Na$^+$]$^+$, 1634 [M + K$^+$]$^+$. UV-vis (CHCl$_3$): λ_{max} (10^{-3} ε) 245 (60), 296 (23), 351 (9.0), 453 (6.5), 499 nm (36 dm^3 mol^{-1} cm^{-1}).

FeBd$_2$(CwGm)(BF)$_2$ (12). Bis[2-(*o*-oxyphenoxy)]diethyl ether (0.41 g, 1.43 mmol) was added to a solution of sodium methoxide, prepared from metallic sodium (0.07 g, 3.0 mmol) and dry methanol (15 ml). The reaction mixture was refluxed for 30 min and evaporated to dryness, and solid residue was left at 90–100 °C for 1 h *in vacuo*. The resulting salt and complex **6** (1.0 g, 1.3 mmol), along with the interphase carrier (*n*-Bu$_4$N)Cl (0.36 g), were dissolved/suspended in dry THF (100 ml) at −20 °C. The reaction mixture was stirred for 2 h at this temperature and for 5 h at 50 °C, cooled to room temperature and filtered. The filtrate was evaporated to dryness. The solid was washed with water, methanol, a small amount of diethyl ether and then with hexane. The chloroform solution of the product obtained was filtered through Silasorb SPH-300 and evaporated to dryness, dissolved in chloroform–hexane mixture (1 : 1, 50 ml) and filtered. The filtrate was evaporated to dryness, washed with hexane and dried *in vacuo*. Yield: 0.15 g (12%). Anal. calc. for

C$_{46}$H$_{36}$N$_6$O$_{11}$B$_2$F$_2$Fe: C, 57.30; H, 3.74; N, 8.72; Fe, 5.79; found: C, 57.22; H, 3.77; N, 8.63; Fe, 5.87%. MS(PD): m/z 964 [M]$^{+\cdot}$. UV-vis (CHCl$_3$): λ_{max} (10^{-3} ε) 261 (27), 295 (15), 340 (4.6), 437 (7.0), 488 nm (20 dm^3 mol^{-1} cm^{-1}).

FeBd$_2${(MeS)$_2$Gm}$_2$(BF)$_2$ (13). Solutions of *t*-C$_5$H$_{11}$OK (3 ml, 1 M in THF) and MeSH (2 ml, 10% in THF) were added to dry THF (10 ml) under argon and the reaction mixture was cooled to −20 °C. Complex **6** (0.75 g, 1 mmol) was added to the solution, and the reaction mixture was stirred for 2 h at room temperature and refluxed for 2 h. Then 5 ml of solvent was distilled off, the reaction mixture was cooled to room temperature and MeI (0.5 ml) and K$_2$CO$_3$ (0.2 g) were added. After stirring for 2 h, the reaction mixture was diluted with ethanol (10 ml). Acetic acid (0.5 ml) was added and the reaction mixture was heated to boiling point. The dark-orange solid was precipitated with water (5 ml), added dropwise. The reaction mixture was left for 3 h at 0 °C and filtered. The product was washed with ethanol and hexane, dried *in vacuo* and dissolved in chloroform. The solution was filtered through Silasorb SPH-300 and evaporated to dryness. Yield: 0.58 g (76%). Anal. calc. for C$_{32}$H$_{26}$N$_6$O$_6$B$_2$F$_2$FeS$_2$: C, 49.90; H, 3.38; N, 10.92; Fe, 7.25; found: C, 49.92; H, 3.33; N, 10.87; Fe, 7.21%. MS(PD): m/z 770 [M]$^{+\cdot}$. UV-vis (CHCl$_3$): λ_{max} (10^{-3} ε) 258 (26), 291 (17), 321 (4.0), 391 (4.2), 486 nm (27 dm^3 mol^{-1} cm^{-1}).

FeBd$_2${(*n*-OctS)$_2$Gm}(BF)$_2$ (14). A solution of *t*-C$_5$H$_{11}$OK (2 ml, 1 M in THF) and *n*-C$_8$H$_{17}$SH (*n*-OctSH, 0.38 ml, 2.2 mmol) were dissolved in dry THF (10 ml) under argon. The complex FeBd$_2$(Cl$_2$Gm)(BF)$_2$ (0.75 g, 1 mmol) was added, and the reaction mixture was stirred for 3 h at room temperate and refluxed for 2 h. The solid product was precipitated with dilute acetic acid (50 ml, 2% in water) and dissolved in chloroform. The dried chloroform solution was filtered through Silasorb SPH-300 and evaporated to *ca.* 1.5 ml. The orange product was precipitated with pentane, washed with pentane and dried *in vacuo*. Yield: 0.56 g (62%). Anal. calc. for C$_{46}$H$_{54}$N$_6$O$_6$B$_2$F$_2$-FeS$_2$: C, 57.18; H, 5.59; N, 8.70; Fe, 5.78; S, 6.63; found: C, 57.02; H, 5.51; N, 8.68; Fe, 5.70; S, 6.53%. MS(PD): m/z 966 [M]$^{+\cdot}$. UV-vis (CHCl$_3$): λ_{max} (10^{-3} ε) 245 (17), 286 (17), 378 (3.7), 484 nm (26 dm^3 mol^{-1} cm^{-1}).

X-Ray crystallography

Details of the crystal data collection and refinement parameters for $FeBd_2(Cl_2Gm)(BF)_2 \cdot 2C_6H_6$ (**6**), $FeBd_2\{(Et_2N)ClGm\}(BF)_2 \cdot C_6H_6$ (**9**) and $FeBd_2\{(MeS)_2Gm\}(BF)_2$ (**13**) complexes are listed in Table 3. Single crystals of these complexes were grown from benzene–iso-octane (**6** and **9**) and methylene dichloride–heptane (**13**) mixtures at room temperature.

Single-crystal X-ray diffraction experiments for complexes **6** and **9** were carried out with a Bruker SMART 1K CCD area detector mounted on a 3-circle diffractometer, using graphite monochromated Mo-Kα radiation (λ = 0.71073 Å). The data collection nominally covered a hemisphere of reciprocal space[40] by a combination of three sets of ω scans (step 0.3°), each set at different φ angles ($2\theta_{max}$ = 60 and 55° for crystals **6** and **9**, respectively). The temperature was maintained with a Cryo-stream open-flow N_2 gas cryostat (Oxford Cryosystems). Reflection intensities were integrated using SAINT software[40] and corrected for absorption by semi-empirical method (SADABS program[41]) based on multiple measurements of identical reflections and Laue equivalents. Data for a single crystal of clathrochelate **13** were collected at 293 K on a CAD4 diffractometer using Mo-Kα (β-filtered) radiation (λ = 0.71073 Å) with $\theta/2\theta$ scans ($2\theta_{max}$ = 52°).

The structures were solved by the direct method and refined by full-matrix least squares against F^2 of all data, using SHELXTL software.[42] Non-hydrogen atoms were refined with anisotropic displacement parameters and hydrogen atoms with isotropic ones for all structures, where a riding model was used. In **9**, there were some residual peaks of electron density, which were situated near the nitrogen atom of the diethylamine group and might be due to unresolved disorder of this fragment. The nonequivalence of the C–N bond lengths in this group and the large anisotropic displacement parameters probably have the same cause. The unit cells of structures **6** and **9** contain one crystallographically independent molecule of the clathrochelate and a solvent benzene in a general position. The molecule of complex **13** is situated in a special position on the 2-fold axis.

CCDC reference numbers 163718–163720.

See http://www.rsc.org/suppdata/dt/b1/b107021p/ for crystallographic data in CIF or other electronic format.

References

1 Ya. Z. Voloshin, O. A. Varzatskii, T. E. Kron, V. K. Belsky, V. E. Zavodnik, N. G. Strizhakova and A. V. Palchik, *Inorg. Chem.*, 2000, **39**, 1907.
2 Ya. Z. Voloshin, O. A. Varzatskii, A. V. Palchik, A. I. Stash and V. K. Belsky, *New J. Chem.*, 1999, **23**, 355.
3 K. E. Erkkila, D. T. Odom and J. K. Barton, *Chem. Rev.*, 1999, **99**, 2777.
4 L. A. Basile and J. K. Barton, *J. Am. Chem. Soc.*, 1987, **109**, 7548.
5 A. A. Bhuiyan and J. R. Kincaid, *Inorg. Chem.*, 1999, **38**, 4759.
6 R. B. Nair, B. M. Cullum and C. J. Murphy, *Inorg. Chem.*, 1997, **36**, 962.
7 E. J. C. Olson, D. Hu, A. Hörmann, A. M. Jonkman, M. R. Arkin, E. D. A. Stemp, J. K. Barton and P. F. Barbara, *J. Am. Chem. Soc.*, 1997, **119**, 11458.
8 P. R. Ashton, R. Ballardini, V. Balzani, E. C. Constable, A. Credi, O. Kocian, S. J. Langford, J. A. Preece, L. Prodi, E. R. Schofield, N. Spencer, J. F. Stoddart and S. Wenger, *Chem. Eur. J.*, 1998, **4**, 2413.
9 D. Burdinski, E. Bothe and K. Wieghardt, *Inorg. Chem.*, 2000, **39**, 105.
10 S. I. Khab, A. E. Beilshtein, M. Sykora, G. D. Smith, X. Hu and M. W. Grinstaff, *Inorg. Chem.*, 1999, **38**, 3922.
11 M. K. Robbins, D. W. Naser, J. L. Heiland and J. J. Grzybowski, *Inorg. Chem.*, 1985, **24**, 3381.
12 J. G. Muller and K. J. Takeuchi, *Polyhedron*, 1989, **8**, 1391.
13 K. L. Bieda, A. L. Kranitz and J. J. Grzybowski, *Inorg. Chem.*, 1993, **32**, 4209.
14 J. J. Grzybowski, R. Daniel Allen, J. A. Belinski, K. L. Bieda, T. A. Bish, P. A. Finnegan, M. L. Hartenstein, C. S. Regitz, D. M. Ryalls, M. E. Squires and H. J. Thomas, *Inorg. Chem.*, 1993, **32**, 5266.
15 C. Engtrakul, W. J. Shoemaker and J. J. Grzybowski, *Inorg. Chem.*, 2000, **39**, 5161.
16 P. Chaudhuri, M. Winter, B. P. C. Della Vedova, P. Fleischhauer, W. Haase, U. Flörke and H.-J. Haupt, *Inorg. Chem.*, 1991, **30**, 4777.
17 D. Burdinski, F. Birkelbach, T. Weyhermüller, U. Flörke, H.-J. Haupt, M. Lengen, A. X. Trautwein, E. Bill, K. Wieghard and P. Chaudhuri, *Inorg. Chem.*, 1998, **37**, 1009.
18 F. Birkelbach, U. Flörke, H.-J. Haupt, C. Butzlaff, A. X. Trautwein, K. Wieghard and P. Chaudhuri, *Inorg. Chem.*, 1998, **37**, 2000.
19 N. A. Kostromina, Ya. Z. Voloshin and A. Y. Nazarenko, *Clathrochelates: Synthesis, Structure, Properties*; Naukova Dumka, Kiev, 1992.
20 N. V. Gerbeleu, V. B. Arion and F. J. Burgess, *Template Synthesis of Macrocyclic Compounds*, Wiley-VCH, Weinheim, 2000.
21 Ya. Z. Voloshin, O. A. Varzatskii, A. V. Palchik, E. V. Polshin, Y. A. Maletin and N. G. Strizhakova, *Polyhedron*, 1998, **17**, 4315.
22 S. V. Linderman, Yu. T. Struchkov and Ya. Z. Voloshin, *Inorg. Chim. Acta*, 1991, **184**, 107.
23 Ya. Z. Voloshin, T. E. Kron, V. K. Belsky, V. E. Zavodnik, Y. A. Maletin and S. G. Kozachkov, *J. Organomet. Chem.*, 1997, **536/537**, 207.
24 Ya. Z. Voloshin, M. I. Terekhova, Y. G. Noskov, V. E. Zavodnik and V. K. Belsky, *An. Quim., Int. Ed.*, 1998, **94**, 142.
25 S. V. Linderman, Yu. T. Struchkov and Ya. Z. Voloshin, *Pol. J. Chem.*, 1993, **67**, 1575.
26 V. E. Zavodnik, V. K. Belsky, Ya. Z. Voloshin and O. A. Varzatsky, *J. Coord. Chem.*, 1993, **28**, 97.
27 Ya. Z. Voloshin, S. V. Linderman and Yu. T. Struchkov, *Koord. Khim.*, 1990, **16**, 1367.
28 V. E. Zavodnik, V. K. Belsky, Ya. Z. Voloshin and O. A. Varzatsky, *Pol. J. Chem.*, 1993, **67**, 1567.
29 S. A. Kubow, K. J. Takeuchi, J. J. Grzybowski, A. J. Jircitano and V. L. Goedken, *Inorg. Chim. Acta*, 1996, **241**, 21.
30 Ya. Z. Voloshin, N. A. Kostromina and A. Yu. Nazarenko, *Inorg. Chim. Acta*, 1990, **170**, 181.
31 A. Yu. Nazarenko, E. V. Polshin and Ya. Z. Voloshin, *Mendeleev Commun.*, 1993, 45.
32 A. M. Bond, K. B. Oldham and C. G. Zoski, *J. Electroanal. Chem.*, 1988, **245**, 71.
33 R. J. Tait, P. C. Bury, B. C. Finnin, B. L. Reed and A. M. Bond, *Anal. Chem.*, 1993, **65**, 3252.
34 A. J. Bard and L. R. Faulkner, *Electrochemical Methods: Fundamentals and Applications*, 2nd ed., Wiley, New York, 2001.
35 E. P. Kyba, R. C. Helgeson, K. Maden, G. M. Gokel, T. L. Tarnowski, S. S. Moore and D. J. Cram, *J. Am. Chem. Soc.*, 1977, **59**, 2564.
36 L. A. Tchugaev, *Zh. Russ. Fiz. Khim. O–va., Chast Khim.*, 1909, **41**, 184.
37 G. Ponzio and F. Baldrocco, *Gazz. Chim. Ital.*, 1930, **60**, 415.
38 A. N. Nekrasov and V. V. Yutchenko, SPECTRA Program, Karpov Institute of Physical Chemistry, Moscow, Russia, 1996.
39 D. W. Thompson and D. V. Stynes, *Inorg. Chem.*, 1990, **29**, 3815.
40 SMART and SAINT, release 5.0, Area Detector Control and Integration Software, Bruker AXS, Inc., Madison, WI, USA, 1998.
41 G. M. Sheldrick, SADABS: Program for Exploiting the Redundancy of Area Detector X-Ray Data, University of Göttingen, Germany, 1999.
42 G. M. Sheldrick, SHELXTL, version 5.1, Programs for the Solution and Refinement of Crystal Structures, Bruker AXS, Inc., Madison, WI, USA, 1997.